ISSN: 2832-4293

Pan-American Journal of Mathematics 5 (2026), 2
https://doi.org/10.28919/cpr-pajm/5-2

SPATIOTEMPORAL COMPLEXITY OF A SELF- AND CROSS-DIFFUSIONS PREDATOR-PREY SYSTEM WITH IVLEV FUNCTIONAL RESPONSE

ABDULLAH ALDURAYHIM[1], SANAA MOUSSA SALMAN[2], AMR ELSONBATY[1,3], ABDULKARIM A. ABDULRAZZAK[4], AND A.A. ELSADANY[1,5,*]

ABSTRACT. This paper examines the emergence of complex dynamics in a predator-prey system characterized by the Ivlev functional response and influenced by both self- and cross-diffusion. We analytically derive the conditions for the occurrence of Hopf, Turing, and wave bifurcations within a spatially extended domain. Additionally, we provide a theoretical investigation into the evolutionary processes that shape the spatial distribution and interactions of populations undergoing local diffusion. Through numerical simulations, we uncover a diverse range of spatiotemporal patterns, including spots, spirals, and other regular and irregular structures. Our results reveal that the inclusion of spatial effects leads to richer and more intricate dynamics, such as irregular behavior and spiral wave formation. These insights contribute to a deeper understanding of the ecological dynamics.

1. INTRODUCTION

Ecological systems inherently involve complex interactions between species and their environments, often across various spatial and temporal scales. Since the foundational work of Lotka and Volterra in the 1920s [1,2], which introduced the now-classic predator–prey model with its characteristic cycles, such models have remained central to both ecology and mathematical biology due to their broad applicability and significance.

Pattern formation in nonlinear complex systems is a cornerstone of research in different natural and biological systems [3]. Beginning with the foundational studies of Segel and Jackson [4], researchers have observed that spatial patterns and population aggregation commonly emerge in ecological systems, driven by localized interactions in both natural settings and theoretical models. The field expanded significantly after Turing's groundbreaking analysis of reaction-diffusion systems [5], which established a key theoretical foundation for studying pattern formation across multiple disciplines. In recent years, reaction-diffusion

[1]MATHEMATICS DEPARTMENT, COLLEGE OF SCIENCE AND HUMANITIES STUDIES IN AL-KHARJ, PRINCE SATTAM BIN ABDULAZIZ UNIVERSITY, AL-KHARJ 11942, SAUDI ARABIA

[2]MATHEMATICS DEPARTMENT, FACULTY OF EDUCATION, ALEXANDRIA UNIVERSITY, ALEXANDRIA, EGYPT

[3]MATHEMATICS AND ENGINEERING PHYSICS DEPARTMENT, FACULTY OF ENGINEERING, MANSOURA UNIVERSITY, P.O. 35516, MANSOURA, EGYPT

[4]MEDICAL INSTRUMENTATION TECHNIQUES ENGINEERING DEPARTMENT, COLLEGE OF TECHNICAL ENGINEERING, URUK UNIVERSITY, IRAQ

[5]DEPARTMENT OF BASIC SCIENCE, FACULTY OF COMPUTERS AND INFORMATICS, ISMAILIA 41522, SUEZ CANAL UNIVERSITY, EGYPT

E-mail addresses: am.aldurayhim@psau.edu.sa, samastars9@gmail.com, a.elsonbaty@psa.edu.sa, abdulkarimAAbdulrazzak@gmail.com, aelsadany1@yahoo.com.

Submitted on Nov. 15, 2025.

2020 *Mathematics Subject Classification.* Primary 39A60, 35K51; Secondary 35C07, 35K58.

Key words and phrases. Predator-prey system; Ivlev-type functional response; Stability; Bifurcation; Turing pattern formation.

*Corresponding author.

models have seen increasing use due to their capacity to capture intricate spatial dynamics in fields like biology [6-10], chemistry [11–12], and physics [13-15]. These models serve as vital tools for investigating how simple, localized interactions can give rise to complex, often self-organized, large-scale patterns in diverse systems.

Recently, many researchers have explored predator–prey models with various functional responses and harvesting strategies. Shang et al. [16] examined the effects of a constant-yield harvesting rate on system stability and bifurcation behavior, showing that constant prey harvesting can destabilize the system. They also found that a linear harvest rate better reflects real-world dynamics. Lian et al. [17] investigated a model with cross-diffusion predator–prey model with nonlinear harvesting term. Their work emphasized the role of harvest intensity in generating population oscillations. To further improve model realism, Shang et al. [18] proposed a predator–prey model with a simplified Holling type IV functional response and a nonlinear Michaelis–Menten-type harvest term. This approach better captured complex ecological interactions and the effects of nonlinear harvesting on system dynamics. Overall, these studies highlight the importance of incorporating harvest terms in predator–prey models to understand ecological systems under human influence and to support more effective resource management strategies.

The following predator-prey system with an Ivlev functional response has gained more attention [19]:

$$\begin{aligned} \dot{u} &= ru(1-u) - (1-e^{-\alpha u})v, \\ \dot{v} &= v[(1-e^{-\alpha u}) - mv - d], \end{aligned} \tag{1.1}$$

where u and v denote prey and predator densities, respectively. The parameters r, α, m and d are all positive and have the following meaning. r is the intrinsic growth rate of the prey, m is the intraspecies competition coefficient, d is the natural death rate of the predator. The term $(1-e^{-\alpha u})$ is the Ivlev type functional response, where α is the conversion rate of consumed prey to predator. In model (1.1), the trophic transfer between species is assumed to be equivalent. The authors in [1] assumed that at different levels in the food chain, the trophic transfer is more complex. Nonlinear trophic transfers with trophic losses should be taken into account. Let $\beta > 0$ be the rate of trophic absorption of predator, then system (1.1) will be in the form:

$$\begin{aligned} \dot{u} &= ru(1-u) - (1-e^{-\alpha u})v, \\ \dot{v} &= v[(1-e^{-\beta u}) - mv - d], \end{aligned} \tag{1.2}$$

with $0 < \beta \leq \alpha$ which means trophic losses in the transfer is taken into account. Assume that the prey is of economic interest, that is it can be harvested, and let the harvesting ratio be proportional to the prey population, then system (1.2) becomes [1]:

$$\begin{aligned} \dot{u} &= ru(1-u) - (1-e^{-\alpha u})v - hu, \\ \dot{v} &= v[(1-e^{-\beta u}) - mv - d]. \end{aligned} \tag{1.3}$$

The authors in [1] assumed that $0 < d < 1$ and $r > h$. In the current paper, the spatiotemporal dynamics of the system (1.3) will be investigated under uniform environment. The interaction between species is modeled by reaction-diffusion systems taking into account the movements of species for food, mates, or shelter. Consider the movement of both prey and predator in the plane, the system under consideration will be in the form:

$$\begin{aligned} \frac{\partial u(x,t,y)}{\partial t} &= ru(1-u) - (1-e^{-\alpha u})v - hu + D_{11}\nabla^2 u, \\ \frac{\partial v(x,t,y)}{\partial t} &= v[(1-e^{-\beta u}) - mv - d] + D_{22}\nabla^2 v, \end{aligned} \tag{1.4}$$

where $u(x,t,y)$ and $v(x,t,y)$ are, respectively, the prey and predator densities at a position $(x,y) \in \Omega \in \mathbb{R}^2_+$ and time t, $D_{11} > 0$, $D_{22} > 0$ are the diffusion coefficients of prey and predator, respectively, and $\nabla^2 = \frac{\partial^2}{\partial x^2} + \frac{\partial^2}{\partial y^2}$ is the Laplacian operator in a two-dimensional space.
In natural, the prey species tend to move away from the predator species in order to protect themselves from the predator's attack. Meanwhile, the predator species approach the higher concentration of the prey species, however, they prefer to avoid group defense. The escape velocity of the prey is proportional to the diffusive velocity of the predator. This phenomena is called cross-diffusion. The main thrust of this paper is to investigate the influence of the cross-diffusion on system (1.4). Consequently, the model we are going to employ takes the form:

$$\begin{aligned} \frac{\partial u(x,y,t)}{\partial t} &= ru(1-u) - (1-e^{-\alpha u})v - hu + D_{11}\nabla^2 u + D_{12}\nabla^2 v, \\ \frac{\partial v(x,y,t)}{\partial t} &= v[(1-e^{-\beta u}) - mv - d] + D_{21}\nabla^2 u + D_{22}\nabla^2 v. \end{aligned} \tag{1.5}$$

The parameters D_{12} and D_{21} are, separately, the cross-diffusion coefficients that describe the population fluxes of prey and predator as a result of the other species's presence. The values of D_{12} imply that the prey populations move towards lower concentration of the predator populations, while the values of D_{21} imply that the predator populations move towards higher concentration of the prey populations. Thus, the values of D_{12} and D_2 might be positive, negative, or zero. We summarize the possible cases for the cross-diffusion parameters as follows.

- If $D_{12} < 0, D_{21} < 0$, then the prey species tends to diffuse to higher concentration areas of the predator species and the predator species tends to diffuse to higher concentration area of the prey species.

- If $D_{12} > 0, D_{21} > 0$, then the prey species tends to diffuse to lower concentration areas of the predator species and the predator species tends to diffuse to lower concentration area of the prey species.

- If $D_{12} < 0, D_{21} > 0$, then the prey species tends to diffuse to higher concentration areas of the predator species and the predator species tends to diffuse to lower concentration area of the prey species.

- If $D_{12} > 0, D_{21} < 0$, then the prey species tends to diffuse to lower concentration areas of the predator species and the predator species tends to diffuse to higher concentration area of the prey species.

In this paper, we assume that the diffusive matrix

$$D = \begin{pmatrix} D_{11} & D_{12} \\ D_{21} & D_{22} \end{pmatrix},$$

is positive definite, that is, $D_{11} > 0, D_{22} > 0$, and we assume that $D_{11}D_{22} - D_{21}D_{12} > 0$, to achieve the principle of thermodynamics, which indicates that self-diffusion is stronger than cross-diffusion.

The system (1.5) is analyzed with the no-flux boundary and nonnegative initial conditions

$$\begin{aligned} \frac{\partial u}{\partial \mathbf{n}} = \frac{\partial v}{\partial \mathbf{n}} = 0, \quad (x,y) \in \partial\Omega, t > 0, \\ u(x,y,0) \geq 0, v(x,y,0) \geq 0, \quad (x,y) \in \Omega, \end{aligned} \tag{1.6}$$

where $\frac{\partial}{\partial \mathbf{n}}$ denotes the derivative along the outward unit normal vector to $\partial\Omega$.

The structure of the paper is as follows. Local dynamics of the temporal system (1.3) is summarized in Section 2. Bifurcation analysis of the spatio-temporal system (1.5) is discussed in Section 3. In Section 4, a series of numerical simulations are performed. The paper ends with a conclusion in Section 5.

2. Local dynamics of the temporal system

In this section, we summarize the local dynamics of the system (1.3) as follows [1].
The system (1.3) has the equilibria:

- $E_0 = (0, 0)$ which means the absence of both the prey and the predator; always exists,
- $E_1 = (1 - \frac{h}{r}, 0)$ which means the existence of the prey in the absence of the predator; exits only if $r > h$,
- $E_* = (u^*, v^*)$ which means the co-existence of both the prey and the predator. This equilibrium point is the unique positive one and it exists only if $d < 1 - e^{-\beta(1-\frac{h}{r})}$ and $\alpha < \frac{2r}{r-h}$. $E_* = (u^*, v^*)$ here satisfies
$$-\frac{1}{\beta}\ln(1-d) < u^* < 1 - \frac{h}{r},\ v^* = \frac{1}{m}(1 - e^{-\beta u^*} - d).$$

In order to study the local stability of the equilibria, we need to calculate the Jacobian matrix of the system (1.3) at any (u, v) which reads

$$J(u,v) = \begin{pmatrix} r(1-2u) - \alpha e^{-\alpha u}v - h & -1 + e^{-\alpha u} \\ \beta v e^{-\beta u} & 1 - d - e^{-\beta u} - 2mv \end{pmatrix}.$$

We summarize the local stability of the equilibria of the system (1.3) in the following proposition.

Proposition 1. *The equilibria of the system (1.3) have the following topological classifications:*

- *E_0 is a saddle point,*
- *E_1 is a sink if $1 - e^{-\beta(1-\frac{h}{r})} < d$ and a saddle if $1 - e^{-\beta(1-\frac{h}{r})} > d$,*
- *E_* is locally asymptotically stable if the following conditions hold true:*

$$d < 1 - e^{-\beta(1-\frac{h}{r})} \text{ and } \alpha < \frac{2r}{r-h}.$$

Proof. The Jacobian matrix calculated at $E_0 = (0, 0)$ reads

$$J(E_0) = \begin{pmatrix} r-h & 0 \\ 0 & -d \end{pmatrix},$$

and the eigenvalues associated to $J(0, 0)$ are $\lambda_1 = r - h > 0$ and $\lambda_2 = -d < 0$. Thus, E_0 is a saddle point. While the Jacobian matrix calculated at $E_1 = (1 - \frac{h}{r}, 0)$ reads

$$J(E_1) = \begin{pmatrix} -r-h & -1 + e^{-\alpha(1-\frac{h}{r})} \\ 0 & 1 - d - e^{-\beta(1-\frac{h}{r})} \end{pmatrix},$$

the eigenvalues associated to $J(E_1)$ are $\lambda_1 = -r - h < 0$ and $\lambda_2 = 1 - d - e^{-\beta(1-\frac{h}{r})}$. If $1 - e^{-\beta(1-\frac{h}{r})} < d$, then E_1 is a sink, while if $1 - e^{-\beta(1-\frac{h}{r})} > d$, then E_1 is a saddle point.
Note that the Jacobian matrix J^* calculated at E_* reads

$$J^* = \begin{pmatrix} r(1-2u^*) - \alpha e^{-\alpha u^*} v^* - h & -1 + e^{-\alpha u^*} \\ \beta v^* e^{-\beta u^*} & -mv^* \end{pmatrix} = \begin{pmatrix} a_{11} & a_{12} \\ a_{21} & a_{22} \end{pmatrix}$$

with trace, $tr(J^*) = a_{11} + a_{22} = r(1-2u^*) - h - mv^* - \alpha e^{-\alpha u^*} v^* < 0$,
and determinant

$$\begin{aligned} det(J^*) &= a_{11}a_{22} - a_{21}a_{12} = -mv^*(r(1-2u^*) - h - \alpha e^{-\alpha u^*} v^*) \\ &- \beta v^* e^{-\beta u^*}(-1 + e^{-\alpha u^*}) > 0. \end{aligned}$$

This means that E_* is locally asymptotically stable. □

The characteristic equation associated to J^* reads

$$\lambda^2 - tr(J^*) + det(J^*) = 0, \tag{2.1}$$

with

$$\lambda_{1,2} = \frac{1}{2}(tr(J^*) \pm \sqrt{tr^2(J^*) - 4det(J^*)}). \tag{2.2}$$

3. Bifurcation analysis of the spatiotemporal system

In this section, we derive cross-diffusion driven instability conditions for the system (1.5) at the interior equilibrium point $E_* = (u^*, v^*)$. According to Turing instability phenomenon [3,5,20], the reaction-diffusion nonlinear system is asymptotically stable in the absence of diffusion but it is unstable if diffusion is present. We will obtain the parametric Turing space conditions under which the aforementioned instability takes place. First of all, we execute a linear stability analysis of the system (1.5) at the interior point E_* for small space- and time-dependent fluctuations and expand u and v in Fourier space as

$$\begin{aligned} u(x,y,t) &\sim u^* + \bar{u}(x,y,t), \quad |\bar{u}(x,y,t)| \ll u^*, \\ v(x,y,t) &\sim v^* + \bar{v}(x,y,t), \quad |\bar{v}(x,y,t)| \ll v^*, \end{aligned} \tag{3.1}$$

where

$$\begin{aligned} \bar{u}(x,y,t) &= \theta_1 e^{\lambda t + i(k_x x + k_y y)}, \\ \bar{v}(x,y,t) &= \theta_2 e^{\lambda t + i(k_x x + k_y y)}, \end{aligned} \tag{3.2}$$

where $\mathbf{k} = (k_x, k_y)$ is the wave number of the solution, $k = |\mathbf{k}| = \sqrt{k_x^2 + k_y^2} \in \mathbb{Z}^+ \cup \{0\}$, $i = \sqrt{-1}$, λ is the perturbation growth rate in time t, θ_1 and θ_2 are the corresponding amplitude. Substituting relations (3.2) into the system (1.5) and neglecting all nonlinear terms in u and v we obtain the following

$$\lambda \begin{pmatrix} \theta_1 \\ \theta_2 \end{pmatrix} = \begin{pmatrix} a_{11} - D_{11}k^2 & a_{12} - D_{12}k^2 \\ a_{21} - D_{21}k^2 & a_{22} - D_{22}k^2 \end{pmatrix} \begin{pmatrix} \theta_1 \\ \theta_2 \end{pmatrix}.$$

Thus, the characteristic equation of the reaction-diffusion system (1.5) reads

$$\lambda^2 - tr_k(J^*)\lambda + det_k(J^*) = 0, \ k \in \mathbb{N}_0 = \{0, 1, 2, ...\}, \tag{3.3}$$

where

$$\begin{aligned} tr_k(J^*) &= -(D_{11} + D_{22})k^2 + tr(J^*), \\ det_k(J^*) &= (D_{11}D_{22} - D_{12}D_{21})k^4 - (a_{11}D_{22} + a_{22}D_{11} - a_{12}D_{21} - a_{21}D_{12})k^2 \\ &+ det(J^*). \end{aligned}$$

The eigenvalues associated to the characteristic equation are

$$\lambda_k = \frac{1}{2}(tr_k(J^*) \pm \sqrt{tr_k^2(J^*) - 4det_k(J^*)}).$$

3.1. **Turing bifurcation.** Turing bifurcation can be achieved for the reaction-diffusion system (1.5) if the equilibrium point E_* which is stable in the absence of diffusion becomes unstable if diffusion is present. From the conditions for local asymptotic stability of the system (1.3) at E_* we know that $tr(J^*) < 0$, this guarantees that $tr_k(J^*)$ is also negative since $tr_k(J^*) = -(D_{11} + D_{22})k^2 + tr(J^*)$. Hence, we E_* loses its stability only when

$$\begin{aligned} det_k(J^*) = A(k^2) &= (D_{11}D_{22} - D_{12}D_{21})k^4 \\ &- (a_{11}D_{22} + a_{22}D_{11} - a_{12}D_{21} - a_{21}D_{12})k^2 \\ &+ det(J^*) < 0. \end{aligned} \tag{3.4}$$

Since we have assumed that $D_{11}D_{22} - D_{12}D_{21} > 0$ and we already have $det(J^*) > 0$, the only necessary condition in which Turing bifurcation may occur is that the coefficient of k^2 in (3.4) must be negative, i.e., $a_{11}D_{22} + a_{22}D_{11} - a_{12}D_{21} - a_{21}D_{12} > 0$. Actually, $A(k^2)$ achieves its minimum at the critical value $k^2 = k_c^2$, where

$$k_c^2 = \frac{a_{11}D_{22} + a_{22}D_{11} - a_{12}D_{21} - a_{21}D_{12}}{2(D_{11}D_{22} - D_{12}D_{21})} > 0. \tag{3.5}$$

The condition $A(k^2) < 0$ at k_c^2 turns into

$$\frac{(a_{11}D_{22} + a_{22}D_{11} - a_{12}D_{21} - a_{21}D_{12})^2}{4(D_{11}D_{22} - D_{12}D_{21})} > det(J^*),$$

which is the Turing instability condition. Note that in the absence of cross diffusion (that is $D_{12} = D_{21} = 0$), the condition for Turing instability becomes

$$a_{11}D_{22} + a_{22}D_{11} > 2\sqrt{det(J^*)D_{11}D_{22}}.$$

Now, in the presence of cross-diffusion, the conditions for the Turing-space are given as follows:

(1) $tr(J^*) = a_{11} + a_{22} < 0$,

(2) $det(J^*) = a_{11}a_{22} - a_{12}a_{21} > 0$,

(3) $D_{11}a_{22} + D_{22}a_{11} - D_{12}a_{21} - D_{21}a_{12} > 0$,

(4) $\frac{(a_{11}D_{22}+a_{22}D_{11}-a_{12}D_{21}-a_{21}D_{12})^2}{4(D_{11}D_{22}-D_{12}D_{21})} > det(J^*)$.

By definition, the first two conditions ensure that the equilibrium point E_* is stable for the non-diffusive system (1.3). For the reaction-diffusion system (1.5), E_* becomes unstable if $Re(\lambda_{1,2}(k^2))$ bifurcates from negative to positive values. In view of the characteristic equation (3.3), a necessary condition for $Re(\lambda_{1,2})(k^2) > 0$ is $det_k(J^*) < 0$, which leads to the last two conditions.
The above four conditions ensure that the stable equilibrium point E_* becomes unstable due to perturbation through wave numbers which are the roots of the equation $A(k^2) = 0$. Hence

$$k_{1,2}^2 = \frac{-\mathcal{B} \pm \sqrt{\mathcal{B}^2 - 4\mathcal{A}\mathcal{C}}}{2\mathcal{A}},$$

where

$$\begin{aligned} \mathcal{A} &= D_{11}D_{22} - D_{12}D_{21}, \\ \mathcal{B} &= a_{11}D_{22} + a_{22}D_{11} - a_{12}D_{21} - a_{21}D_{12}, \\ \mathcal{C} &= det(J^*). \end{aligned}$$

Generally speaking, at the bifurcation point, two equilibria of the model system intersect and exchange their stability. Biologically speaking, this bifurcation means a smooth transition between equilibrium states. In case of Turing bifurcation, the spatial symmetry is broken and spatial pattern are formulated which are stationary in time and oscillatory in space. The equilibria in the Turing space which are stable with respect to homogeneous perturbations lose their stability due to perturbations of specific wave numbers k. Taking r as the bifurcation parameter, the critical value r_T for Turing bifurcation can be obtained by solving the equation $A(k^2) = 0$, hence we obtain

$$r_T = \frac{\theta_1 k^4 + \theta_2 k^2 + mv^*(h + \alpha e^{-\alpha u^*} v^*) - \beta v^* e^{-\beta u^*}(-1 + e^{-\alpha u^*})}{mv^*(1 - 2u^*)}, \tag{3.6}$$

where

$$\begin{aligned} \theta_1 &= D_{11}D_{22} - D_{12}D_{21}, \\ \theta_2 &= -(a_{11}D_{22} + a_{22}D_{11} - a_{12}D_{21} - a_{21}D_{12}). \end{aligned}$$

4. Numerical simulations

In this section, different scenarios for the dynamics of the model are investigated in temporal-only and spatio-temporal cases.

4.1. **Temporal-only dynamics.** In the first scenario, we consider the cases where the steady state of prey only E_1 is locally asymptotically stable. We examine two examples in which the conditions of stability for E_1 are satisfied. Let $r = 0.5; \mathrm{h} = 0.4; d = 0.4; \alpha = 1.3; \beta = 1.55; m = 1$. Fig.1 (a-c) depict that E_1 is stable in this case. Also, let $r = 0.85; \mathrm{h} = 0.8; d = 0.3; \alpha = 1.3; \beta = 1.1; m = 1$. Then, the obtained Fig.1 (d-f) show that the solution orbits converge to the stable E_1. It is important to note that the steady-state value for prey population is very small since the value of harvesting rate in this case is larger than its value in previous case.

In the second scenario, we consider the cases where coexistence steady state E_2 is locally asymptotically stable. Two examples are also presented to confirm the stability conditions obtained E_2. In the first example, the parameters' values are selected as $r = 0.7; \mathrm{h} = 0.2; d = 0.3; \alpha = 1.3; \beta = 1.1; m = 1$. Fig.2 (a-c) shows that E_2 is stable. Also, let $r = 0.6; \mathrm{h} = 0.2; d = 0.3; \alpha = 0.9; \beta = 0.7; m = 1$. Then, the attained Fig.2 (d-f) show that the solution orbits converge to the stable E_2 too.

5. Spatio-temporal dynamics

Numerical evaluations for Turing instability conditions (TICs) are essential due to the complicated forms of these conditions. In particular, we investigate the critical Turing bifurcation value for each parameter in the system when the other parameters are kept fixed.

Let $D_{11} = 0.102; D_{12} = 0.02; D_{21} = 0.08; D_{22} = 0.02$ and consider the following scenarios:

Case I: Parameter r is varied and the remaining parameters are fixed at $\mathrm{h} = 0.2; d = 0.3; \alpha = 0.75; \beta = 0.7; m = 1.5$.

Case II: Parameter α is varied and the remaining parameters are fixed at $r = 0.68; \mathrm{h} = 0.2; d = 0.3; \beta = 0.7; m = 1.5$.

Case III: Parameter h is varied and the remaining parameters are fixed at $r = 0.68; d = 0.3; \alpha = 0.75; \beta = 0.7; m = 1.5$.

Case IV: Parameter m is varied and the remaining parameters are fixed at $r = 0.68; d = 0.3; \alpha = 0.75; \beta = 0.7; h = 0.15$.

Similarly, Case V and Case VI study TICs for parameters d and β, respectively.

The obtained results are presented in Figure 3 to Figure 6 where WOLFRAM MATHEMATICA package are used. Each curve in Figs 3(a), 4(a), 5(a), 6(a) is associated to one of the TICs in the way that Turing space is found when all curves are above zero. The positive initial conditions for the solutions are taken randomly about the homogeneous steady state E_2 of the system within the range $\{E_2 \pm 0.01\}$ and the homogeneous Neumann boundary conditions are employed.

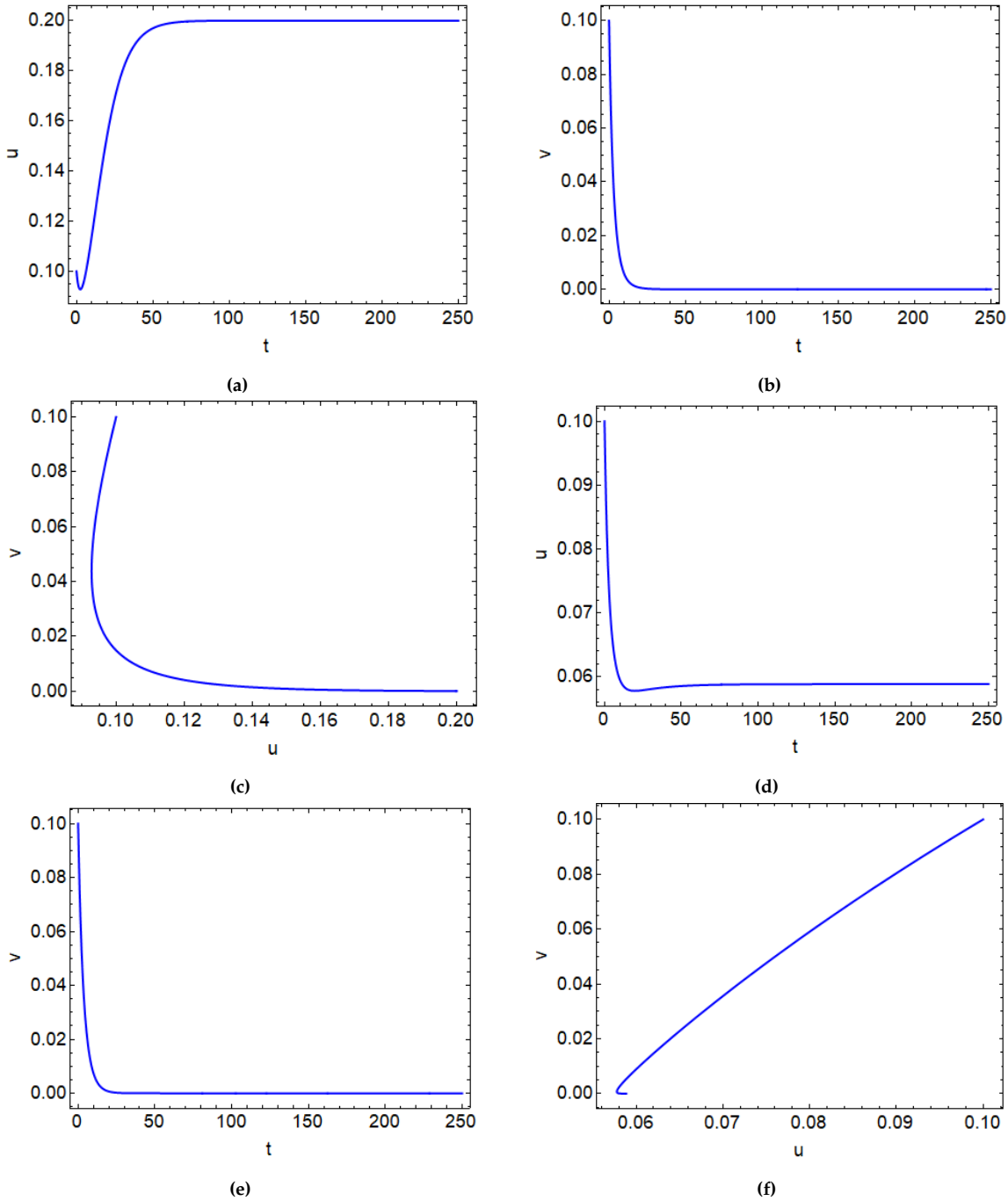

Figure 1. Solution trajectories and phase portraits of the state variables at (a-c) $r = 0.5; \mathrm{h} = 0.4; d = 0.4; \alpha = 1.3; \beta = 1.55; m = 1$ and (d-f) $r = 0.85; \mathrm{h} = 0.8; d = 0.3; \alpha = 1.3; \beta = 1.1; m = 1$.

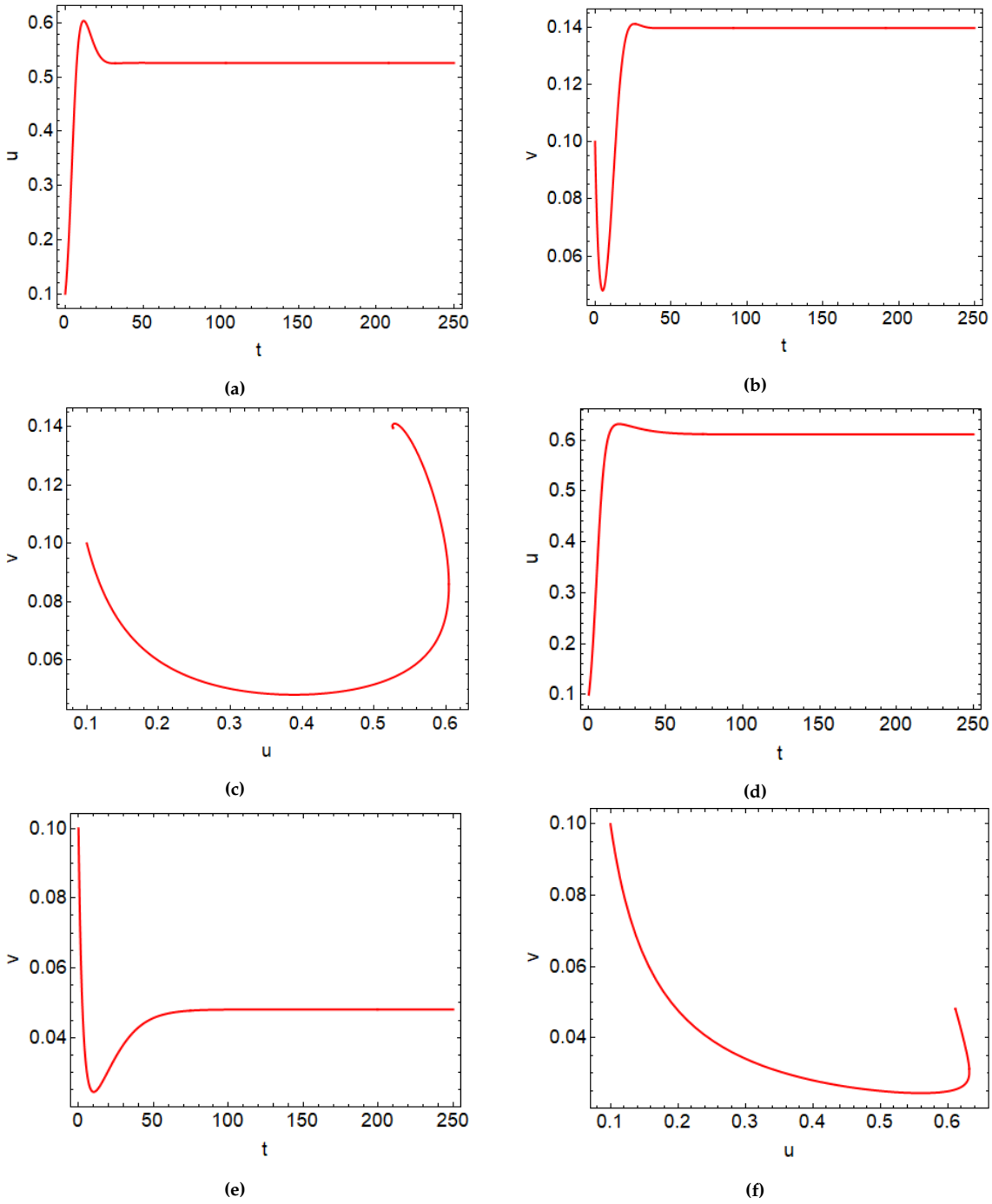

Figure 2. Solution trajectories and phase portraits of the state variables at (a-c) $r = 0.7; \mathrm{h} = 0.2; d = 0.3; \alpha = 1.3; \beta = 1.1$ and (d-f) $r = 0.6; \mathrm{h} = 0.2; d = 0.3; \alpha = 0.9; \beta = 0.7; m = 1$.

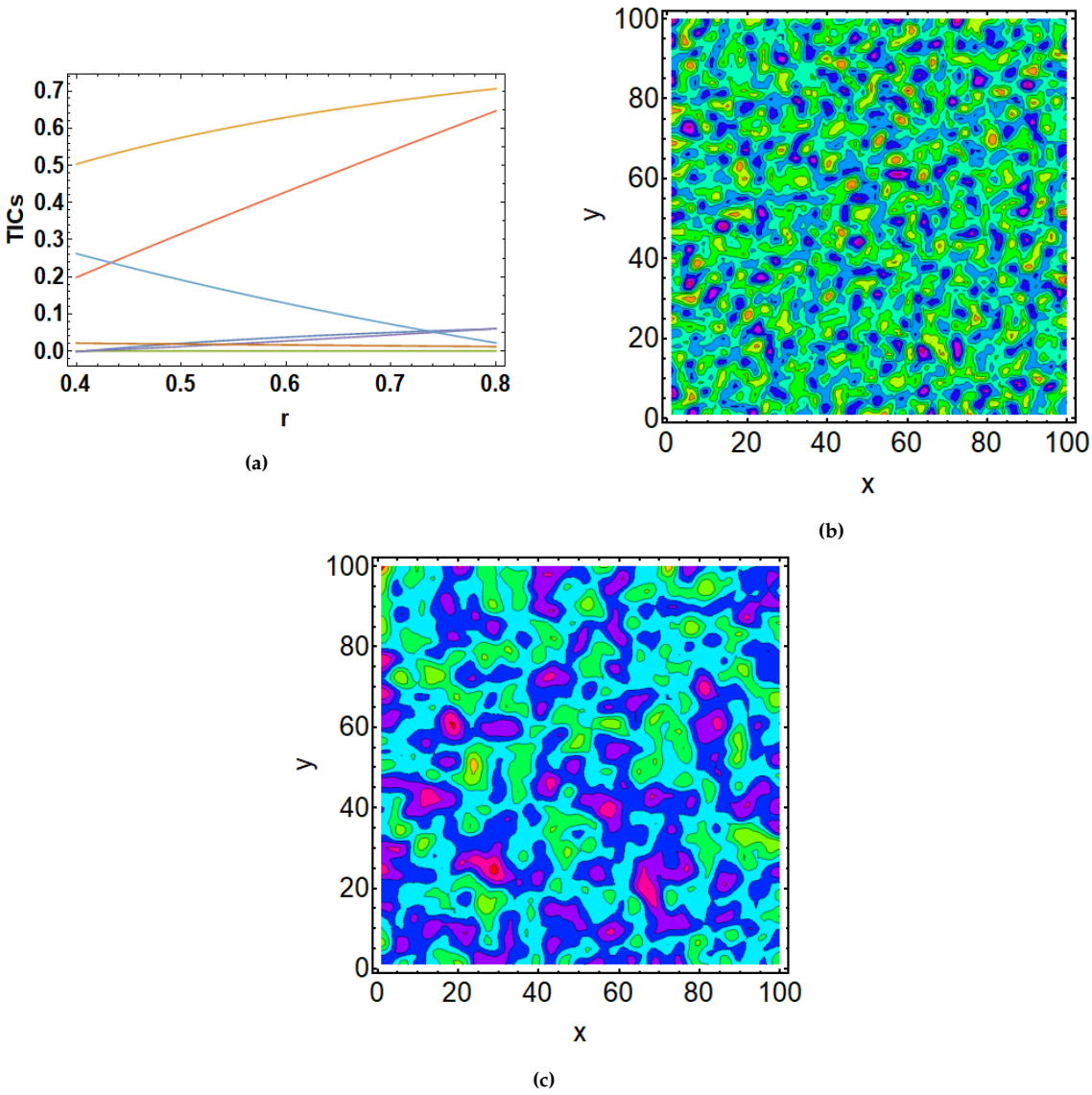

Figure 3. Examination of Turing instability conditions (TICs) in terms of r at h $= 0.2; d = 0.3; \alpha = 0.75; \beta = 0.7; m = 1.5$ in (a) and the obtained Turing patterns for u and v are shown in (b) and (c), respectively, where $r = 0.68$.

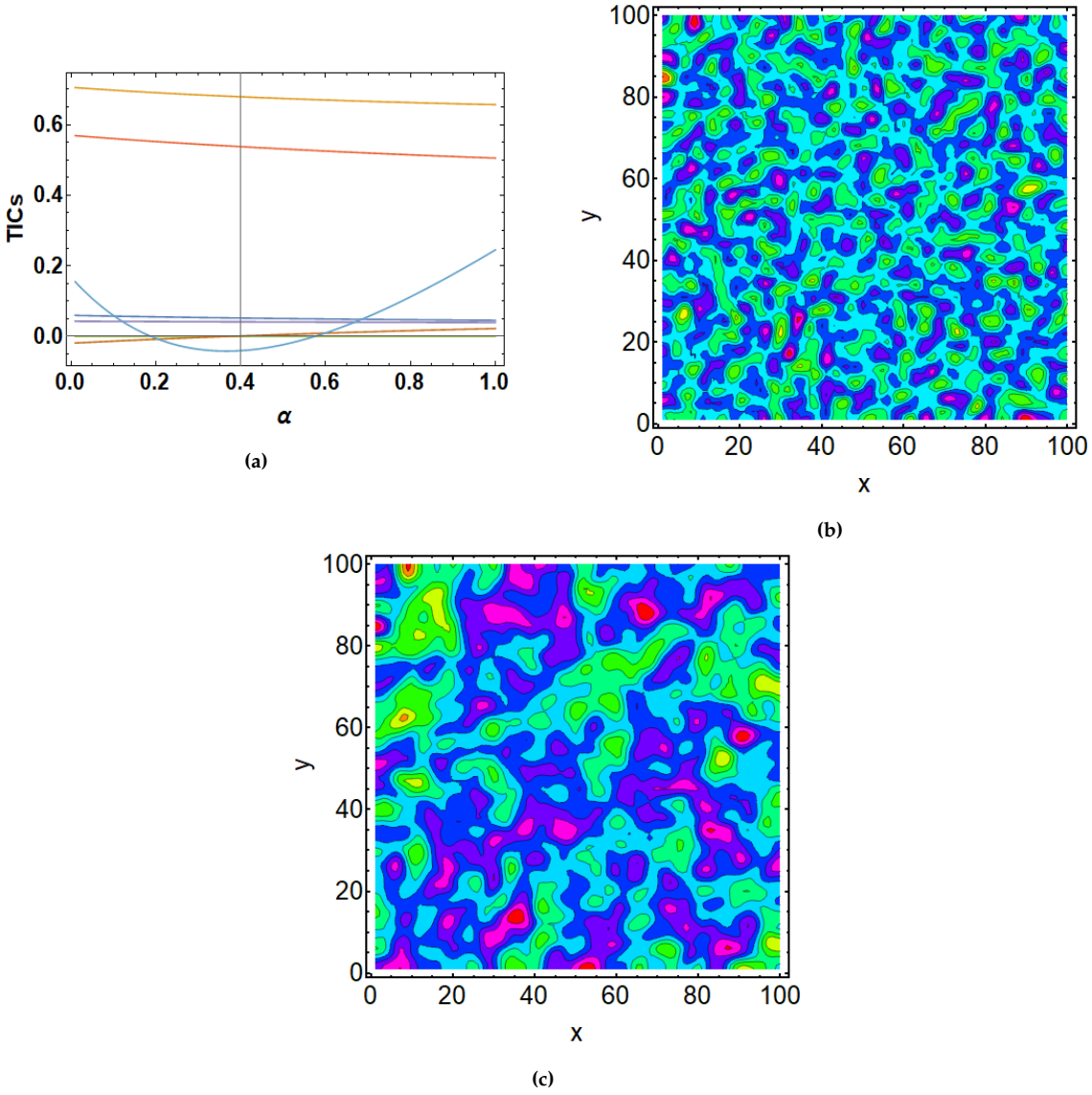

Figure 4. Examination of Turing instability conditions (TICs) in terms of α at $r = 0.68; \mathrm{h} = 0.2; d = 0.3; \beta = 0.7; m = 1.5$ in (a) and the obtained Turing patterns for u and v are shown in (b) and (c), respectively, at $\alpha = 0.73$.

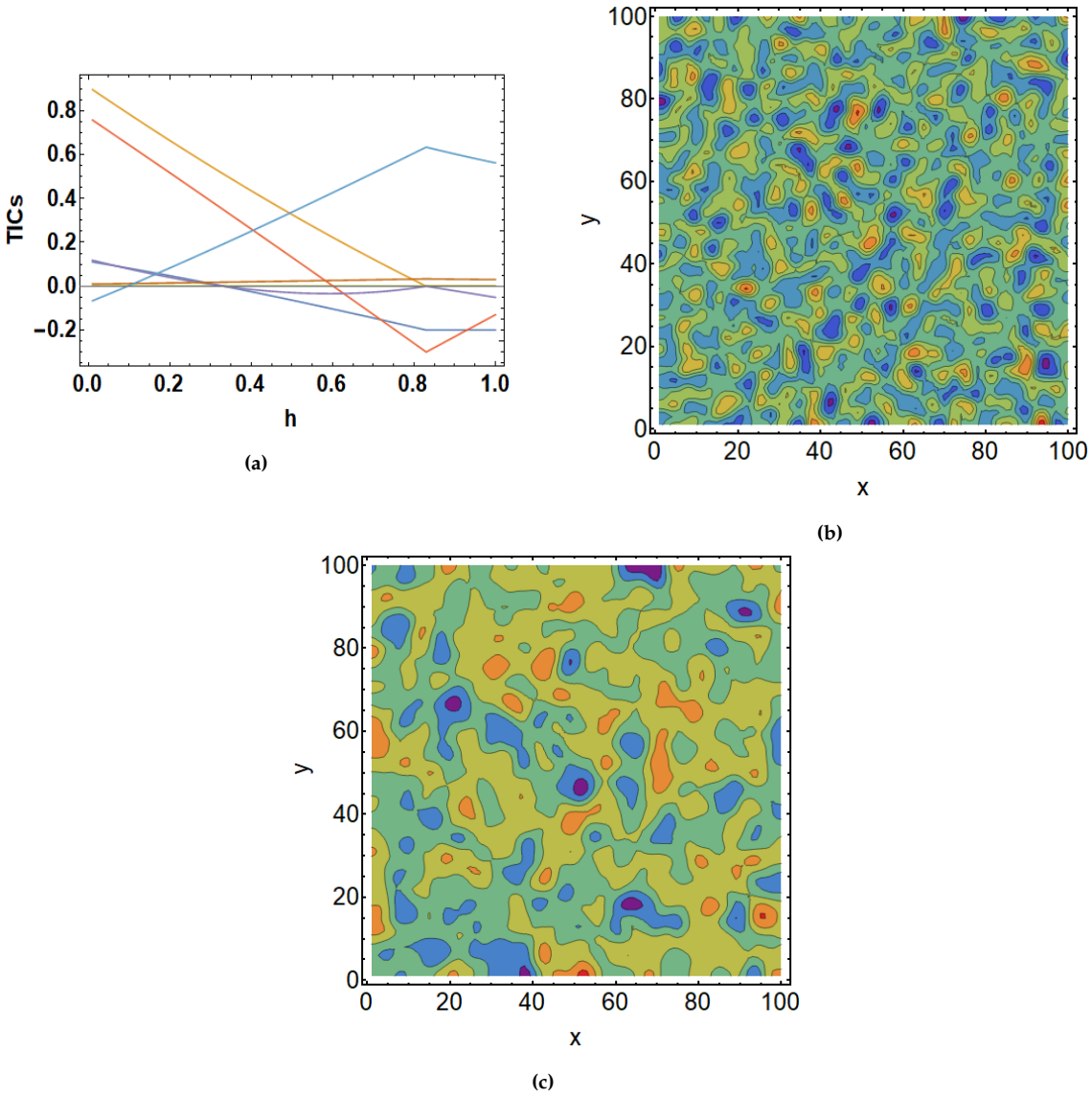

Figure 5. Examination of Turing instability conditions (TICs) in terms of h at $r = 0.68; \alpha = 0.75; d = 0.3; \beta = 0.7; m = 1.5$; in (a) and the obtained Turing patterns for u and v are shown in (b) and (c), respectively, at $h = 0.15$.

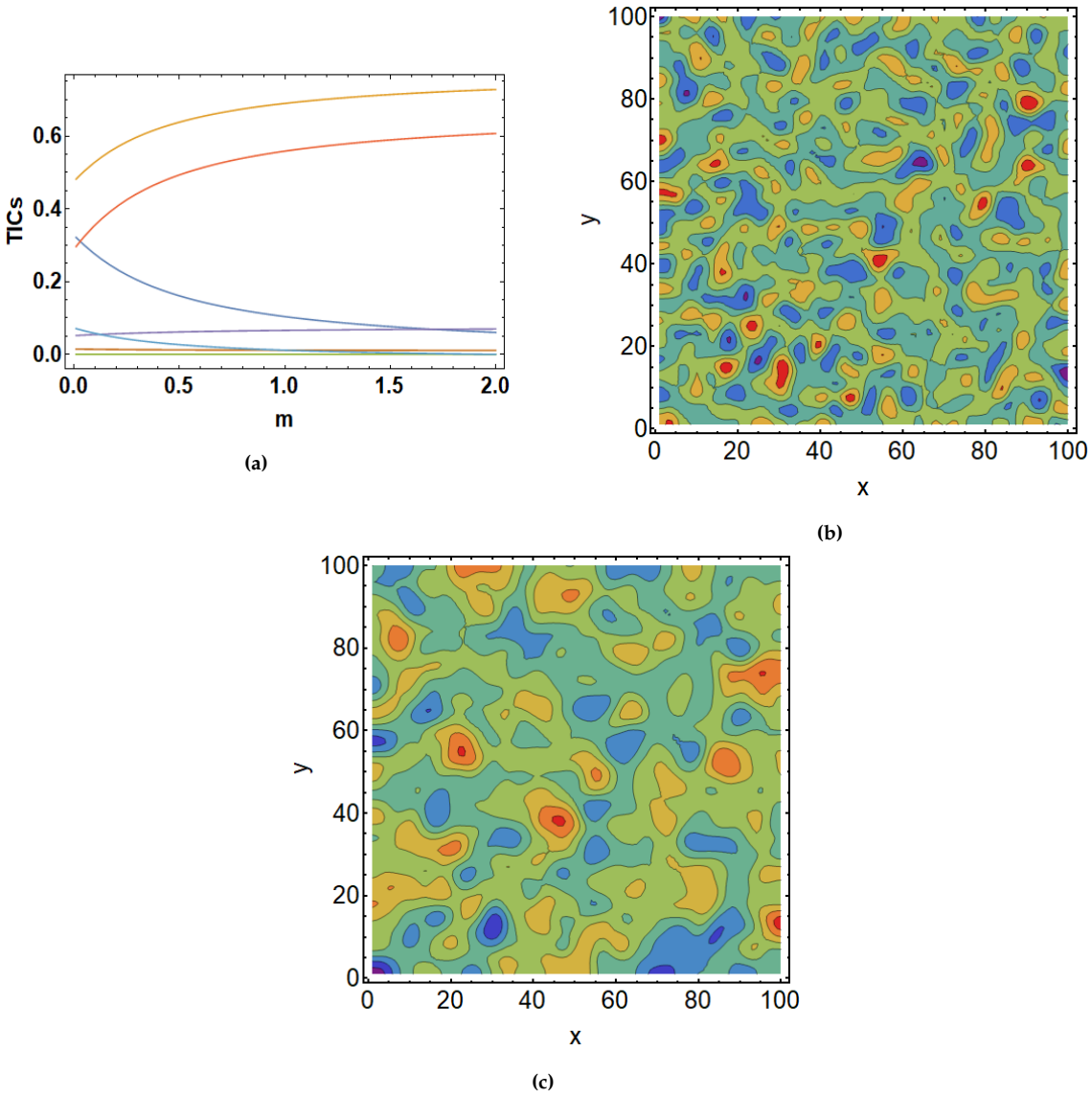

Figure 6. Examination of Turing instability conditions (TICs) in terms of m at $r = 0.68; \alpha = 0.75; \mathrm{h} = 0.15; d = 0.3; \beta = 0.75$ in (a) and the obtained Turing patterns for u and v are shown in (b) and (c), respectively, at $m = 0.9$.

6. Conclusions and discussions

This study investigates pattern formation in a predator-prey system governed by self-diffusion and cross-diffusion, incorporating the Ivlev functional response. We analyze the conditions for Hopf, Turing, and wave bifurcations, assessing system stability through eigenvalue analysis and the Routh–Hurwitz criterion. By comparing scenarios with and without cross-diffusion, we demonstrate how varying diffusion coefficients drive transitions between distinct spatial patterns holes, hole strip mixtures, stripes, and spots.

Our findings reveal that cross-diffusion is a critical factor in shaping these patterns. To isolate the role of cross-diffusion, we first examined pattern evolution in its absence, observing that the system consistently stabilized into a hole pattern. Introducing cross-diffusion—with coefficients D_{12} and D_{21} as key parameters triggered a progression from holes to hybrid hole-strip formations. Further increases in D_{12} shifted patterns toward pure stripes, while adjustments to parameters r, α, m and h ultimately produced spot patterns. These results highlight how cross-diffusion coefficients profoundly influence spatiotemporal dynamics, yielding diverse and complex structures. Notably, initial irregular patterns consistently evolved into stable, ordered configurations (holes, hole-strips, stripes, or spots), indicating system wide convergence to equilibrium. Additionally, numerical simulations revealed that spiral wave patterns, generated under varied initial conditions, maintained consistent structures regardless of starting configurations further evidence of stability. Beyond spirals, the system exhibited a rich array of patterns, including mosaics, spots, and chaotic arrangements. These findings illustrate how species interactions and spatial movement generate persistent ecological patterns, offering insights into real-world predator-prey dynamics and their observable spatial structures.

Funding. The corresponding author is supported via funding from Prince Sattam bin Abdulaziz University project number (PSAU/2025/R/1447).

Competing interests. The authors declare no competing interests.

References

[1] A.J. Lotka, Elements of Mathematical Biology, Williams and Wilkins, Baltimore, (1925).

[2] V. Volterra, Variazioni e Fluttuazioni del Numero di' Individui in Specie Animali Conviventi, Mem. R. Accad. Naz. Dei Lincei, Ser. VI 2 (1926), 31–113.

[3] J.D. Murray, Mathematical Biology. II Spatial Models and Biomedical Applications, Springer (2001).

[4] L.A. Segel, J.L. Jackson, Dissipative Structure: An Explanation and an Ecological Example, J. Theor. Biol. 37 (1972), 545–559. https://doi.org/10.1016/0022-5193(72)90090-2.

[5] A.M. Turing, The Chemical Basis of Morphogenesis, Philos. Trans. R. Soc. Lond. Ser. B, Biol. Sci. 237 (1952), 37–72. https://doi.org/10.1098/rstb.1952.0012.

[6] C. Ou, J. Wu, Spatial Spread of Rabies Revisited: Influence of Age-Dependent Diffusion on Nonlinear Dynamics, SIAM J. Appl. Math. 67 (2006), 138–163. https://doi.org/10.1137/060651318.

[7] K. Sarkar, S. Khajanchi, Spatiotemporal Dynamics of a Predator-Prey System with Fear Effect, J. Frankl. Inst. 360 (2023), 7380–7414. https://doi.org/10.1016/j.jfranklin.2023.05.034.

[8] S. Khajanchi, J.J. Nieto, Spatiotemporal Dynamics of a Glioma Immune Interaction Model, Sci. Rep. 11 (2021), 22385. https://doi.org/10.1038/s41598-021-00985-1.

[9] M. Chen, R. Wu, Steady States and Spatiotemporal Evolution of a Diffusive Predator–Prey Model, Chaos Solitons Fractals 170 (2023), 113397. https://doi.org/10.1016/j.chaos.2023.113397.

[10] M. Yaremenko, Holder Solvability of Quasi-Linear Parabolic Systems in the Divergent Form, Pan-Amer. J. Math. 3 (2024), 2. https://doi.org/10.28919/cpr-pajm/3-2.

[11] A.C. Redfield, The Biological Control of Chemical Factors in the Environment. Am. Sci. 46 (1958), 205–221. https://www.jstor.org/stable/27827150.

[12] G. Becker, H. Holfeld, A.T. Hasselrot, D.M. Fiebig, D.A. Menzler, Use of a Microscope Photometer to Analyze in Vivo Fluorescence Intensity of Epilithic Microalgae Grown on Artificial Substrata, Appl. Environ. Microbiol. 63 (1997), 1318–1325. https://doi.org/10.1128/aem.63.4.1318-1325.1997.

[13] D. Walgraef, Spatio-Temporal Pattern Formation: With Examples from Physics, Chemistry, and Materials Science, Springer, (2012). https://doi.org/10.1007/978-1-4612-1850-0.

[14] L.A. Peletier, W.C. Troy, Spatial Patterns: Higher Order Models in Physics and Mechanics, Springer, (2012). https://doi.org/10.1007/978-1-4612-0135-9.

[15] A.L. Krause, E.A. Gaffney, T.J. Jewell, V. Klika, B.J. Walker, Turing Instabilities Are Not Enough to Ensure Pattern Formation, Bull. Math. Biol. 86 (2024), 21. https://doi.org/10.1007/s11538-023-01250-4.

[16] Y. Shang, M. Kasada, M. Kondoh, Interplay of Trophic Relaxation and Directional Selection Shapes Eco-evolutionary Responses to Selective Harvest in Predator–Prey Systems, Oikos 2025 (2025), e11463. https://doi.org/10.1002/oik.11463.

[17] X. Lian, H. Wu, M. Zhu, W. Xu, Pattern Dynamics of a Cross-Diffusion Predator–Prey Model with Nonlinear Harvesting Term, Adv. Contin. Discret. Model. 2025 (2025), 60. https://doi.org/10.1186/s13662-025-03921-z.

[18] Z. Shang, Y. Qiao, L. Duan, J. Miao, Stability and Bifurcation Analysis in a Nonlinear Harvested Predator–Prey Model with Simplified Holling Type IV Functional Response, Int. J. Bifurc. Chaos 30 (2020), 2050205. https://doi.org/10.1142/s0218127420502053.

[19] C. Zhang, L. Liu, P. Yan, L. Zhang, Stability and Hopf Bifurcation Analysis of a Predator-Prey Model with Time Delayed Incomplete Trophic Transfer, Acta Math. Appl. Sin. Engl. Ser. 31 (2015), 235–246. https://doi.org/10.1007/s10255-015-0463-7.

[20] Y.A. Kuznetsov, Elements of Applied Bifurcation Theory, Springer, New York, 1998. https://doi.org/10.1007/b98848.